Cherenkov radiation based antenna with the funnel-shaped directional pattern

Petro Melezhik, Michel Ney, Seil Sautbekov, Kostyantyn Sirenko, Yuriy Sirenko, Alexey Vertiy & Nataliya Yashina

Taylor & Francis
Taylor & Francis Group

Check for updates

Cherenkov radiation based antenna with the funnel-shaped directional pattern

Petro Melezhik[a], Michel Ney[b], Seil Sautbekov[c], Kostyantyn Sirenko [a], Yuriy Sirenko[a,c], Alexey Vertiy[c], and Nataliya Yashina[a]

[a]Mathematical Physics Department, O. Usikov Institute for Radiophysics and Electronics of National Academy of Sciences of Ukraine, Kharkiv, Ukraine; [b]Département Micro-Ondes, Lab-STICC/Telecom Bretagne, Technopôle Brest-Iroise, Brest Cedex 3, France; [c]Radiophysics and Electronics Department, L. Gumilyov Eurasian National University, Astana, Kazakhstan

ABSTRACT

An axially symmetric diffraction antenna of a new type is presented and studied in details in the paper. The antenna is based on the effect of Cherenkov-like radiation. In contrast to diffraction antennas presented earlier, the proposed antenna does not contain periodic structures, which are effortful in manufacturing for millimetre and shorter waves. The antenna consists of a dielectric-filled cylindrical waveguide which feeds a biconical dielectric prism. Simulation results show that the proposed antenna has high efficiency, low sidelobe level, and the radiation pattern with high directivity. The proposed antenna could be used in various communication and radar systems.

Introduction

Modern challenges of mm-wave systems put new requirements to antenna construction and characteristics. Some of the related challenges could be efficiently alleviated utilizing diffraction radiation antennas (diffraction antennas; see Yevdokymov 2013; Melezhik et al. 2010; Sautbekov et al. 2015; Rusch et al. 2015; and Sirenko and Velychko 2016), which transform the field of surface waves of any open line into volume outgoing waves. In such antennas, a periodic structure is typically used for converting the near field of a guiding structure into radiation. During the last 50 years, the development and implementation of experimental and theoretical methods of design and analysis of such structures have advanced substantially (see for instance Sirenko and Strom 2010). Over the past years, dozens of radar, radiometric, and terrestrial and aerospace-based communication systems have been reported. Their operation is greatly facilitated using the unique characteristics of diffraction antennas (Melezhik et al. 2010; Yevdokymov 2013).

Naturally, with the shortening of the operating wavelength in a basic design of diffraction antennas (the system of 'open dielectric waveguide – grating') various changes had to be introduced. Most of them were facilitated by the theoretical study of new open guiding structures and arrays, and the efficient way to transform the energy of surface waves (even without distorting the phase characteristics of the field in emitting aperture). Several approaches were developed and successfully exploited. First of all, the method of analytical

regularization (Shestopalov et al. 1997; Sirenko and Strom 2010), the method of integral equations (Colton and Kress 1983), the finite-difference time-domain method (FDTD, see Taflove and Hagness 2000; Berenger 1996), the finite element method (FEM, see Jin 2002; Liu, Sirenko, and Bagci 2012), which allow one to turn gratings (and many other electromagnetic structures) into adequate objects of mathematical modeling. Next, methods utilizing the spectral theory of open resonant structures (Sirenko and Strom 2010; Velychko and Sirenko 2009), which provide extensive accurate study of various eigen regimes. Finally, a method based on exact absorbing conditions (EAC-method, see Hagstrom 1999; Sirenko 2003; Shafalyuk, Sirenko, and Smith 2011; and Sirenko and Velychko 2016), which properly bounds computation domains of open electromagnetic problems and removes numerous restrictions on material and geometric parameters of analyzed structures. The EAC-method addresses important practical problems of electromagnetics, electronics, and optics, in which the essential role is played by the processes of anomalous and resonance spatial-temporal and spatial-frequency transformations of the electromagnetic field.

In this paper, we present a simple model of axially symmetric diffraction antenna based on the effect of Cherenkov-like radiation (Bodrov et al. 2009; Theuer et al. 2006; Melezhik et al. 2006; and Granet et al. 2015). In the presented antenna, not a grating, but a compact scatterer is used as a converter of the near field of an open guiding structure into radiation. Inside the scatterer, electromagnetic waves propagate slower than the guiding structure's surface wave which excites them.

All analysis is carried out by the EAC-enabled FDTD method. All physical parameters are in SI units, except the time t which is measured in meters, t is the product of a real time by the speed of light in vacuum. Dimensions are omitted in the text.

Model problem of the EAC-method

The EAC-method reduces an original open problem (domain of analysis extends to infinity) for an axially symmetric radiating structure (Figure 1) to the following equivalent problem on a bounded domain (Sirenko and Velychko 2016; Shafalyuk, Sirenko, and Smith 2011):

$$
\begin{cases}
\left[-\varepsilon(g) \frac{\partial^2}{\partial t^2} - \sigma(g) \eta_0 \frac{\partial}{\partial t} + \frac{\partial^2}{\partial z^2} + \frac{\partial}{\partial \rho} \left(\frac{1}{\rho} \frac{\partial}{\partial \rho} \rho \right) \right] U(g,t) = 0; \quad t > 0, \quad g \in \Omega_{\text{int}} \\
U(g,t)|_{t=0} = 0, \quad \frac{\partial}{\partial t} U(g,t)|_{t=0} = 0; \quad g = \{\rho, z\} \in \bar{\Omega}_{\text{int}} \\
\vec{E}_{tg}(q,t), \quad \vec{H}_{tg}(q,t) \quad \text{are continuous when crossing } \Sigma^{\varepsilon,\sigma}, \\
\vec{E}_{tg}(p,t)|_{q=\{\rho,\phi,z\} \in \Sigma} = 0, \quad U(0,z,t) = 0 \quad \text{for} \quad \{0,z\} \in \bar{\Omega}_{\text{int}}, \\
D_1 \left[U(g,t) - U_p^{i(1)}(g,t) \right] \Big|_{g \in \Gamma_1} = 0, \quad D_2[U(g,t)]|_{g \in \Gamma_2} = 0, \\
\text{and} \quad D[U(g,t)]|_{g \in \Gamma} = 0; \quad t \geq 0.
\end{cases}
\tag{1}
$$

It is assumed that the structure is fed from the circular or coaxial waveguide Ω_1 by TE_{0p}-wave ($\partial/\partial\phi \equiv 0$, $E_\rho = E_z = H_\phi \equiv 0$) or TM_{0p}-wave ($\partial/\partial\phi \equiv 0$, $H_\rho = H_z = E_\phi \equiv 0$). $\vec{E}_{tg}(q,t)$ and $\vec{H}_{tg}(q,t)$ are the tangential components of electric and magnetic fields vectors $\vec{E} = \{E_\rho, E_\phi, E_z\}$ and $\vec{H} = \{H_\rho, H_\phi, H_z\}$, $q = \{\rho, \phi, z\}$; ρ, ϕ, z are cylindrical coordinates; $\eta_0 = (\mu_0/\varepsilon_0)^{1/2}$ is the impedance of free space; ε_0 and μ_0 are the electric and magnetic constants of
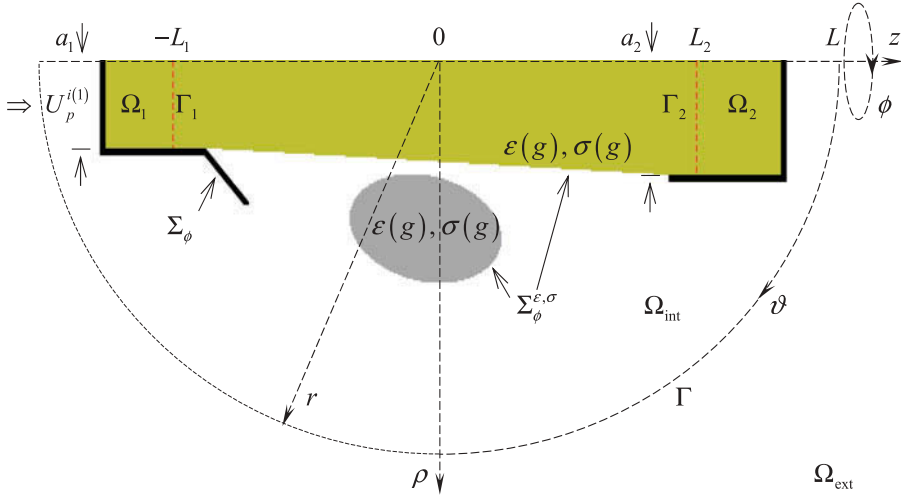
Figure 1. Axially symmetric radiating structure; r, ϑ, φ are spherical coordinates.

vacuum. $U(g, t) = E_\phi(g, t)$ for TE_0-waves and $U(g, t) = H_\phi(g, t)$ for TM_0-waves. The domain of analysis Ω_{int} is a part of the half-plane $\phi = const$ bounded by the contours Σ_ϕ, the virtual boundaries Γ_j, $j = 1, 2$ in the cross-section of the regular waveguides Ω_j, and the virtual boundary $\Gamma = \{g = \{r, \vartheta\} : r = L\}$ in a free space (see Figure 1). The specific conductivity $\sigma(g)$ and the relative permittivity $\varepsilon(g)$ take free space values outside Ω_{int}. All scattering elements, which are set by the piecewise constant functions $\varepsilon(g)$, $\sigma(g)$ and by the piecewise smooth contours Σ_ϕ and $\Sigma_\phi^{\varepsilon,\sigma}$, are located inside Ω_{int}. $\Sigma = \Sigma_\phi \times [0, 2\pi]$ denotes perfectly conducting antenna surfaces, and $\Sigma^{\varepsilon,\sigma} = \Sigma_\phi^{\varepsilon,\sigma} \times [0, 2\pi]$ denotes surfaces on which the functions $\varepsilon(g)$ and $\sigma(g)$ are changing in a step-wise manner.

Explicit forms of the EAC operators $D_1\left[U(g, t) - U_p^{i(1)}(g, t)\right]$, $D_2[U(g, t)]$ and $D[U]$ are presented in (Sirenko and Velychko 2016; Shafalyuk, Sirenko, and Smith 2011). These operators allow one to reduce the computation domain to the bounded region Ω_{int} without changing the infinite domain solution. The waves going out from Ω_{int} cross the virtual boundaries Γ_j and Γ without any distortion or reflection as if the outgoing waves are absorbed completely by these boundaries. The waves propagate in such a way that Ω_1 and Ω_2 may be considered as regular semi-infinite waveguides.

The function

$$U_p^{i(1)}(g, t) = v_{p1}(z, t)\mu_{p1}(\rho); \ g = \{\rho, z\} \in \Omega_1, \ p \geq 0 \text{ is integer}, \tag{2}$$

which is a part of EAC for the virtual boundary Γ_1, defines the pulse TE_{0p}- or TM_{0p}-wave exciting the antenna. It must satisfy the wave equation and the causality principle. This function, or more precisely, values of its amplitudes $v_{p1}(z, t)$ on the boundary Γ_1, as well as the functions $\varepsilon(g)$, $\sigma(g)$ and the contours Σ_ϕ, $\Sigma_\phi^{\varepsilon,\sigma}$ are assumed to be given. Sets of the transverse eigenfunctions $\mu_{n1}(\rho)$ for both possible types of feeding waveguides (circular and coaxial) and for both possible field polarizations can be found in (Sirenko and Velychko 2016).

In the domain Ω_{ext}, the field $U(g, t)$ is determined by its values on the boundary Γ, which are calculated by solving the problem (1), via exact radiation conditions for outgoing waves presented in (Sirenko and Velychko 2016; Shafalyuk, Sirenko, and Smith 2011).

The EAC-method transforms original open (with unbounded domain of analysis) initial boundary value problems into equivalent closed (with bounded domain of analysis) ones. The EAC-method is an analytical and mathematically rigorous method, its main product is exact absorbing conditions (EACs). In this paper's case, EACs are conditions $D_1\left[U(g,t) - U_p^{i(1)}(g,t)\right]\big|_{g\in\Gamma_1} = 0$, $D_2[U(g,t)]\big|_{g\in\Gamma_2} = 0$, and $D[U(g,t)]\big|_{g\in\Gamma} = 0$ enforced on the virtual boundaries of the computation domain. EACs do not distort physics of processes studied numerically. The most detailed description of the EAC-method, its justification, and results could be found in (Sirenko and Velychko 2016). The EAC-method itself does not solve a problem. The EAC-method regularizes a problem and reduces it to a variant which could be solved numerically using conventional FDTD (Taflove and Hagness 2000) or FEM (Jin 2002) methods. In this paper, we use the EACs-enabled FDTD method to solve the problem (1) numerically, the solution to (1) is obtained as point values of the function $U(g, t)$ on $g \in \overline{\Omega_{\text{int}}} \cup \Omega_{\text{ext}}$ and at time moments $t \in [0, T]$, $T < \infty$. The time-domain solution is converted (using integral transform $\tilde{f}(k) = \int_0^T f(t)\exp(ikt)dt$) into frequency-domain characteristics required for the analysis. Let us list some of them:

- $\{\tilde{E}_x(g,k), \tilde{E}_y(g,k), \tilde{E}_z(g,k)\}$ and $\{\tilde{H}_x(g,k), \tilde{H}_y(g,k), \tilde{H}_z(g,k)\}$, $g \in \overline{\Omega_{\text{int}}} \cup \Omega_{\text{ext}}$ are values of the harmonic field components;

- $R_{np}(k)$ and $T_{np}(k)$ are the transformation coefficients of TE_{0p}- or TM_{0p}-waves coming from the waveguide Ω_1 through the boundary Γ_1 into TE_{0n}- or TM_{0n}-waves reflected into the waveguide Ω_1 and transmitted to the waveguide Ω_2;

- $\eta(k) = 1 - W_{\text{abs}}(k) - \sum_n\left[W_{np}^R(k) + W_{np}^T(k)\right]$ is the efficiency of transformation of the exciting TE_{0p}- or TM_{0p}-wave into the radiation field;

- $D(\vartheta, k, M) = \dfrac{\left|\tilde{\vec{E}}_{tg}(M,\vartheta,k)\right|^2}{\max\limits_{0\le\vartheta\le\pi}\left|\tilde{\vec{E}}_{tg}(M,\vartheta,k)\right|^2}$, $0 \le \vartheta \le 180°$, $K_1 \le k \le K_2$ is the normalized radiation pattern calculated along the arc $r = M \ge L$;

- $\vartheta = \bar{\vartheta}(k)$ is an angle determining the orientation of the main lobe: $D(\bar{\vartheta}(k), k, M) = 1.0$;

- $\vartheta_{0.5}(k)$ is the half-power beam width: $\vartheta_{0.5}(k) = \vartheta^+ - \vartheta^-$, $\bar{\vartheta} \in [\vartheta^-, \vartheta^+]$, where $D(\vartheta^+, k, M) = 0.5$ and $D(\vartheta^-, k, M) = 0.5$.

Here, $k = 2\pi/\lambda > 0$ is a wavenumber (frequency parameter or just frequency), λ is a wavelength in free space, T is an upper time limit within the interval of observation $0 \le t \le T$. For all $t > T$, the function $f(t)$ undergoing the transformation is set to zero. $\tilde{\vec{E}}_{tg}(M, \vartheta, k)$ is a tangential component of harmonic electric field on the cylindrical surface $r = M \ge L$, $W_{\text{abs}}(k)$ is a portion of the energy absorbed in imperfect dielectrics; $W_{np}^T(k)$

$(W_{np}^R(k))$ is a portion of the energy of TE_{0n}- or TM_{0n}-waves transmitted (reflected) into the waveguide Ω_2 (Ω_1). In the framework of the model problem (1), not only the function $\eta(k)$ is calculated, but also values of all its components: $W_{abs}(k)$, $W_{np}^T(k)$ and $W_{np}^R(k)$. This allows to identify and analyze separately such important characteristics of an antenna as the radiation efficiency, the matching level of a feeder with a radiating element, the conversion efficiency of dielectric waveguide surface waves into the radiation field. To enable the calculation of the later characteristics, the waveguide Ω_2 is introduced into the model (in practice, it is often replaced with a matched load).

Discussion of the simulation

The basic element of any diffraction antenna is an open waveguide supporting propagation of surface waves of the correct type with a suitable deceleration rate.

Initial design

For our initial design, we have a segment of a cylindrical dielectric waveguide inserted in a circular metal waveguide (Figure 2). The length of the dielectric waveguide is $d = 17.8$, the radius is $a = 0.52$, the relative permittivity of the material is $\varepsilon = 2.1$. The virtual boundaries Γ_j are situated near the plugged ends of the waveguides Ω_j.

The pulse TE_{01}-wave of the circular waveguide Ω_1 excites the dielectric waveguide. This pulse is given by

$$U_1^{i(1)}(g,t): \quad v_{11}(-L_1,t) = 4\frac{\sin\left[\Delta k\left(t - \tilde{T}\right)\right]}{\left(t - \tilde{T}\right)}\cos\left[\tilde{k}\left(t - \tilde{T}\right)\right]\chi(\bar{T} - t) = F_1(t), \qquad (3)$$

where $\tilde{k} = 7.0$, $\Delta k = 1.5$, $\tilde{T} = 40$, $\bar{T} = 80$; $\chi(...)$ is the Heaviside step function, $\tilde{k}$ is the central frequency, Δk defines the spectral width of the pulse ($\tilde{k} - \Delta k \leq k \leq \tilde{k} + \Delta k$), $\tilde{T}$ and $\bar{T}$ are the pulse time retardation (the arrival time of the principal part of the pulse onto the virtual boundary Γ_1) and its duration, respectively. The wideband pulse (3) covers the frequency band $5.5 \leq k \leq 8.5$ ($0.74 \leq \lambda \leq 1.14$). Values of k are taken from the frequency range within which only the fundamental TE_{01}- eigenmode propagates in the waveguides Ω_j; first cutoff frequencies k_n^+ for TE_{0n}-waves are $k_1^+ \approx 5.08$ and $k_2^+ \approx 9.31$.
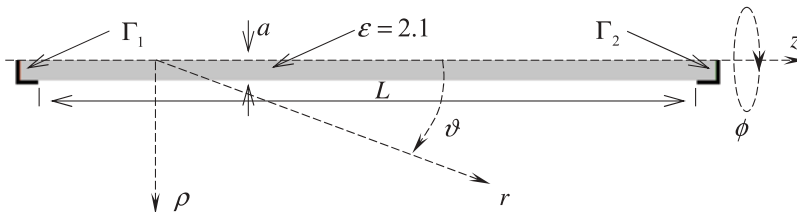

Figure 2. Segment of a circular dielectric waveguide.

Values of $\bar{\chi}(k)$, that is a wavenumber of the slow eigenwave $A(\rho, k) \exp[i\bar{\chi}(k)z]$ of the open waveguide, are obtained (Figure 3) by calculating the phase shift $\zeta(k) = \arg \tilde{E}_\phi(g_2, k) - \arg \tilde{E}_\phi(g_1, k) = \bar{\chi}(k)$ of the field $\tilde{E}_\phi(g, k)$ which occurs while the observation point $g = \{\rho, z\}$ moves along the dielectric waveguide from the point $g = \{\rho, z_1\}$ to the point $g = \{\rho, z_2\}$, $z_2 - z_1 = 1.0$.

From wavenumbers $\bar{\chi}(k)$ of the surface wave, we calculate the moderating coefficient $\gamma(k) = v^{-1}(k) = \bar{\chi}(k)/k$. The function $v(k)$ defines the relative phase velocity of the surface wave. The almost monotonous decrease of $v(k)$ from $v = 0.93$ to $v = 0.80$ is illustrated by Figure 4. Thus, when $k = 7.5$, the function $v(k)$ acquires the value $v = 0.82$.

If we place near the open waveguide a dielectric object made of a material in which the speed of light c is less than v then, according to the Cherenkov radiation theory, waves with quasi-plane front should appear in this object. These waves will propagate at an angle $\theta = \arccos(c/v)$ to the direction of propagation of the surface wave of the dielectric waveguide.

Let that dielectric object be a biconical prism ($\varepsilon_1 = 4.0$, $c = 0.5$) with an inner radius of the hollow cylinder $\Delta = 0.1$ (targeted distance) greater than the radius of the circular dielectric waveguide (Figure 5). There are many ways to attach the prism to the waveguide
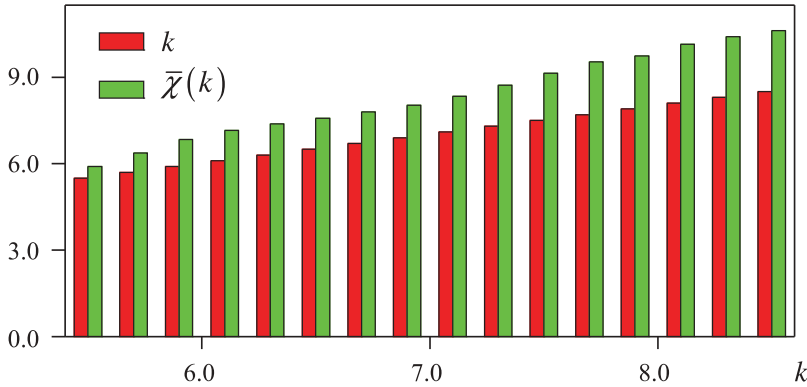

Figure 3. Wavenumbers $\bar{\chi}(k)$ of the surface TE_{01}-wave of the circular dielectric waveguide.
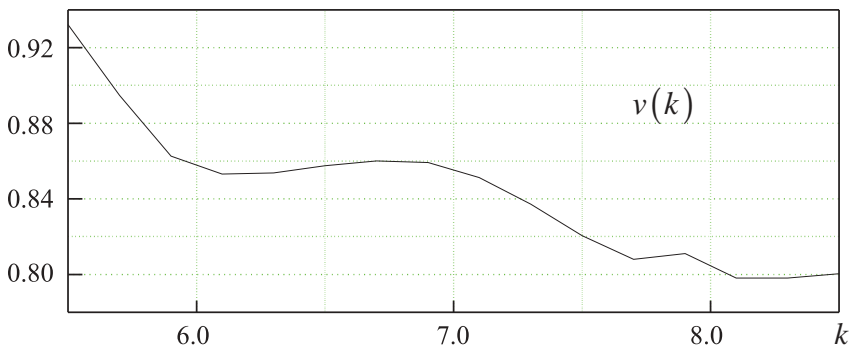

Figure 4. Relative phase velocity of the surface TE_{01}-wave of the circular dielectric waveguide.
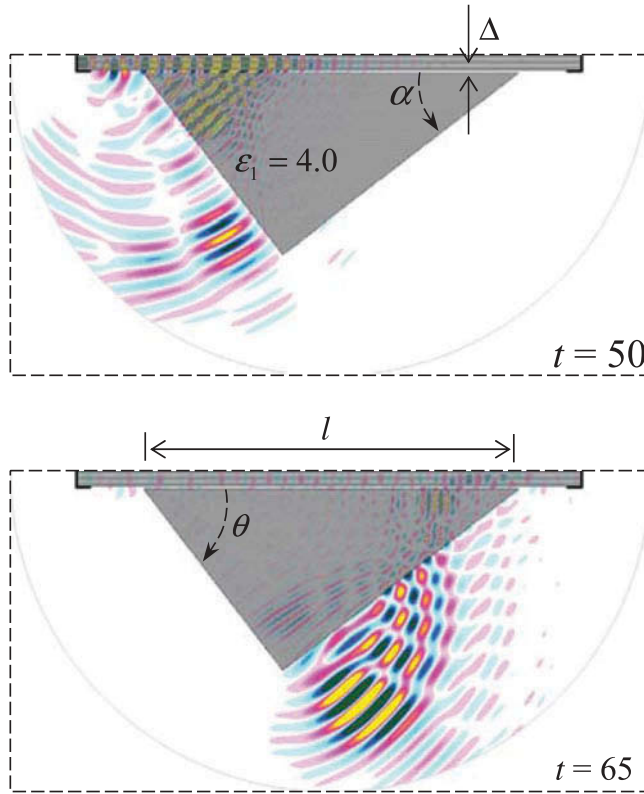
Figure 5. Feeding the initial antenna with the wideband pulse (3). $E_\varphi(g,t)$ pattern at the moments $t = 50$ and $t = 65$.

(e.g., using two dielectric sleeves in the prism at the entrance and exit points of the waveguide), and we do not specify any particular mount in this paper. But we would like to note that any possible mount could be modeled and taken into account using the presented EAC-method. The apex angle of the prism right cone is $\alpha = 37.57°$ (see Figure 5). The apex angle of the left cone is $\theta = 52.43°$. The geometry of the object is designed so that the Cherenkov radiation on the frequency $k = 7.5$ ($v(k) = 0.82$) is parallel to the prism left facet. The total length of the prism is $l = 14.0$.

Exciting this antenna by the pulse (3) with the operation frequency $k = 7.5$ and the frequency band $5.5 \leq k \leq 8.5$ yields the radiation pattern $D(\vartheta, k, \infty)$ and the efficiency $\eta(k)$ shown in Figure 6. One can observe in Figures 5 and 6 that a plane wave front is not obtained in the expected direction, the directivity is rather low, and the sidelobe level is high. Some modifications are required to improve the antenna characteristics.

Modified antenna

First of all, it is necessary to neutralize several local scattering centers on the transitions from the feeding waveguide Ω_1 to the dielectric waveguide with dielectric prism, and from the dielectric waveguide to the waveguide Ω_2. These centers give rise to diverging toroidal waves which significantly reduce the radiation directivity. The second important step is to
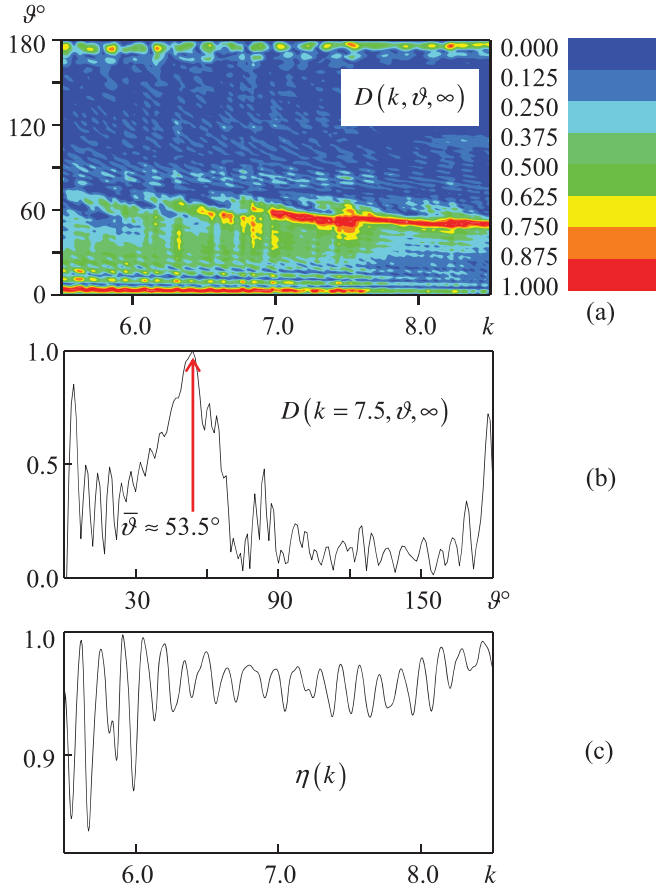
Figure 6. Feeding the initial antenna with the wideband pulse (3). Normalized radiation pattern (a) in the band $5.5 \leq k \leq 8.5$, and (b) on the frequency $k = 7.5$; (c) the efficiency $\eta(k)$.

ensure the uniform power takeoff from the surface wave traveling along the dielectric waveguide by a quasi-plane wave arising in the dielectric prism. This power takeoff should not distort phase characteristics of the surface wave, which are closely related with the wavenumbers $\bar{\chi}(k)$ and the phase velocity $v(k)$.

The suggested modifications are following: the left cone of the prism is covered with a metal surface connected to a horn transition to the waveguide Ω_1; the gap distance along the prism is not constant and varies linearly from $\Delta = 0.26$ to $\Delta = 0.1$; the waveguide Ω_2 is equipped with a smooth horn transition.

Now we discuss the performance of the modified antenna (see Figure 7). Let the antenna is excited by the following narrowband TE_{01}-pulse:

$$U_1^{i(1)}(g, t): \quad v_{11}(-L_1, t) = P(t) \cos\left[\tilde{k}(t - \tilde{T})\right] \chi(\bar{T} - t) = F_2(t);$$

$$\tilde{k} = 7.5, \quad P(t) = 0.01 - 5 - 95 - 99, \quad \tilde{T} = 0.5. \tag{4}$$
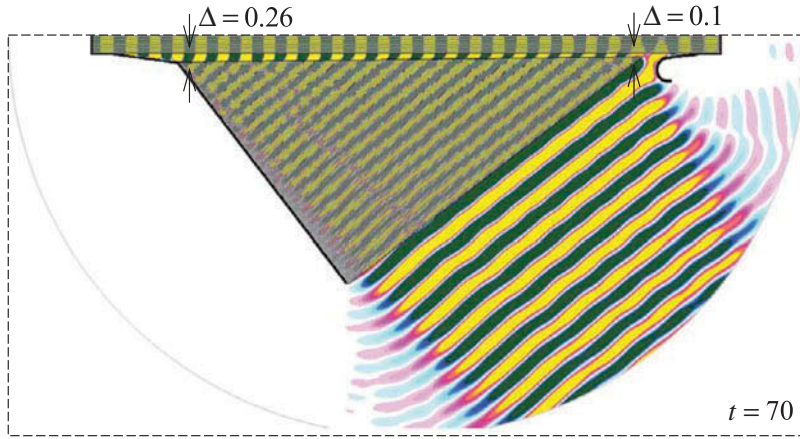
Figure 7. Feeding the modified antenna with the narrowband pulse (4). $E_\varphi(g, t)$ pattern at the moment $t = 70$.

Here, $\tilde{k}$ is the central frequency, $\tilde{T}$ is the delay time, $P(t) = P(t) : t_1 - t_2 - t_3 - t_4$ is a trapezoidal envelope function which vanishes for $t < t_1$ and $t > t_4$, and has unit value for $t_2 < t < t_3$.

The pattern $D(k, \vartheta, \infty)$ and the efficiency $\eta(k)$ calculated in the band $7.45 \leq k \leq 7.55$ and for $k = 7.5$ are shown in Figure 8. The radiation pattern exhibits a much better directivity with rather low side lobes and the efficiency remains high. In Figure 7, one can clearly observe plane waves radiated from the cone side. On the frequency $k = 7.5$, the main lobe is directed at $\bar{\vartheta}(k) = 52.5°$ that differs from the expected ($\bar{\vartheta} = \theta$) only by 0.07°. This result mainly provided by the insignificancy of phase distortions of the field of surface wave caused by its interaction with the dielectric prism. According to the definition from (Sautbekov et al. 2015), in the case discussed, these distortions are less than 1.0° within the whole length of the interaction region. The main lobe width is $\vartheta_{0.5} = 6.0°$, the side lobe is directed at 59.5°, the side lobe level is 0.2 (− 14dB). Computing average value of the function $\bar{\theta} \approx 52.5°$ (Figure 8c) within the interval $0 \leq \vartheta \leq 180°$, we find the maximum directivity $D_{max} \approx 16.3$ and the gain $G = D_{max} \cdot \eta \approx 15.2$ on the frequency $k = 7.5$. The bandwidth of k covered by the data presented in the first two fragments in Figure 8 is about 1.4%. Within this interval, the antenna characteristics stay practically unchanged. More specifically, within the band $7.1 < k < 7.7$, a change of the frequency k by $\pm 1\%$ (or ± 0.075) leads to a change in the phase velocity $v(k)$ of ∓ 0.005, and hence, to a change of the angles θ and $\bar{\vartheta}$ of approximately $\mp 0.27°$. The data presented in Figure 4 allow us to state that in this frequency range, there is a fairly broad band $6.1 \leq k \leq 7.1$ (15% bandwidth) in which the orientation of the main lobe $\bar{\vartheta}(k)$ remains almost constant.

The presented results confirm the possibility to achieve directional radiation patterns for antennas based on the Cherenkov-like radiation. It is clear how and within what limits, it is possible to control the basic characteristics of this type of antennas. Namely, by changing either the type of an open waveguide structure (or the parameters of a surface wave supported by a structure) or the geometric and material parameters of an object from which waves can be radiated into free space.
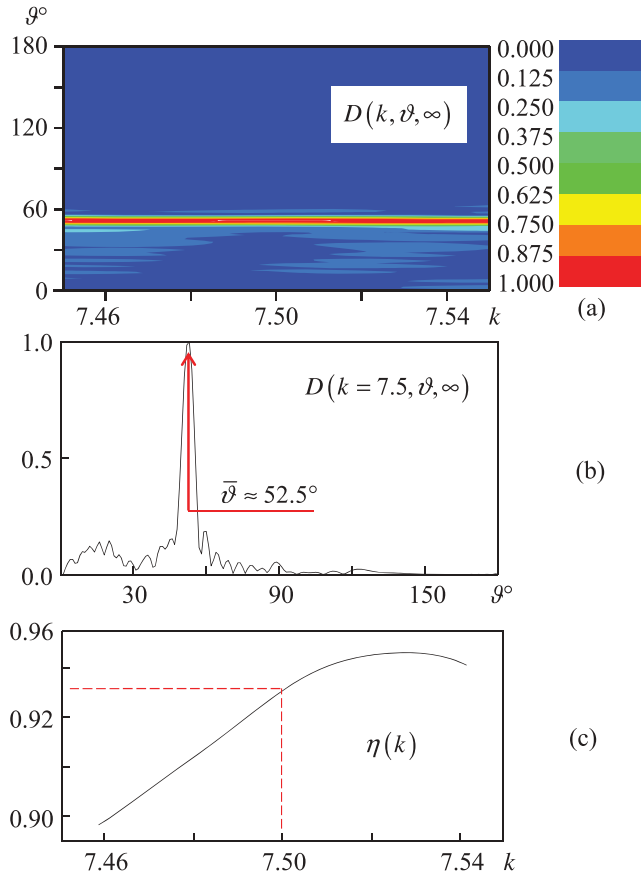
Figure 8. Feeding the modified antenna with the narrowband pulse (4). Normalized radiation pattern (a) in the band $7.45 \leq k \leq 7.55$, and (b) on the frequency $k = 7.5$; (c) the efficiency $\eta(k)$.

Conclusion

An efficient and reliable mathematical model and numerical algorithm were used to design a directional diffraction antenna based on the Cherenkov-like radiation. The antenna consists of a dielectric-filled cylindrical waveguide which feeds a biconical dielectric prism. Simulation results show that a careful design leads to the radiation pattern with relatively high directivity (less than 10° beamwidth), high constant efficiency, and a relatively low sidelobe level. Further optimization is possible using the approach presented in the paper. Theoretical results obtained using the presented approach were repeatedly confirmed by real-world experiments (Sautbekov et al. 2015), comparing with results of other authors (Sirenko and Velychko 2016), and clear and undisputed interpretation of physical effects under study. The results' reliability and authenticity are ensured by rigorous mathematical derivations and mandatory tests of conservation laws, reciprocity relations and so on (Sirenko and Velychko 2016).

ORCID

Kostyantyn Sirenko ⬡ http://orcid.org/0000-0001-8401-2022

References

Berenger, J.-P. 1996. Three-dimensional perfectly matched layer for absorption of electromagnetic waves. Journal Computation Physics 127 (2):363–79.

Bodrov, S., A. Stepanov, M. Bakunov, B. Shishkin, I. Ilyakov, and R. Akhmedzhanov. 2009. Highly efficient optical-to-terahertz conversion in a sandwich structure with LiNbO3 core. Optics Express 17 (3):1871–79.

Colton, D., and R. Kress. 1983. Integral equation methods in scattering theory. New York: Wiley-Interscience.

Granet, G., P. Melezhik, A. Poyedinchuk, S. Sautbekov, Y. Sirenko, and N. Yashina. 2015. Resonances in reverse Vavilov-Cherenkov radiation produced by electron beam passage over periodic interface. International Journal Antennas Propagation 2015:784204.

Hagstrom, T. 1999. Radiation boundary conditions for the numerical simulation of waves. Acta Numerica 8:47–106.

Jin, J. 2002. The finite element method in electromagnetics. New York: John Wiley & Sons.

Liu, M., K. Sirenko, and H. Bagci. 2012. An efficient discontinuous Galerkin finite-element method for highly accurate solution of Maxwell equations. IEEE Transactions Antennas Propagation 60 (8):3992–98.

Melezhik, P., A. Poyedinchuk, N. Yashina, G. Granet, and M. Ney. 2006. Radiation from surface with periodic boundary of metamaterials excited by a current. Progress Electromagnetics Research 65:1–14.

Melezhik, P., Y. Sidorenko, S. Provalov, S. Andrenko, and S. Shilo. 2010. Planar antenna with diffraction radiation for radar complex of millimeter band. Radioelectronics Communication Systems 53 (5):233–40.

Rusch, C., J. Schäfer, H. Gulan, P. Pahl, and T. Zwick. 2015. Holographic mmw-antennas with TE0 and TM0 surface wave launchers for frequency-scanning FMCW-radars. IEEE Transactions Antennas Propagation 63 (4):1603–13.

Sautbekov, S., K. Sirenko, Y. Sirenko, and A. Yevdokymov. 2015. Diffraction radiation effects: A theoretical and experimental study. IEEE Antennas Propagation Magazine 57 (5):73–93.

Shafalyuk, O., Y. Sirenko, and P. Smith. 2011. Simulation and analysis of transient processes in open axially-symmetrical structures: Method of exact absorbing boundary conditions. Chap. 5 in Electromagnetic waves, ed. V.Zhurbenko. Rijeka, Croatia: InTech.

Shestopalov, V., Y. Tuchkin, A. Poyedinchuk, and Y. Sirenko. 1997. New solution methods for direct and inverse problems of the diffraction theory. Analytical regularization of the boundary value problems in electromagnetic theory. Kharkiv: Osnova.(in Russian)

Sirenko, Y. 2003. Exact "absorbing" conditions in outer initial boundary-value problems of the electrodynamics of nonsinusoidal waves. Part 3: Compact inhomogeneities in free space. Telecommunications Radio Engineering 59 (1&2):1–31.

Sirenko, Y., and S. Strom, eds. 2010. Modern theory of gratings. New York: Springer.

Sirenko, Y., and L. Velychko, eds. 2016. Electromagnetic waves in complex systems. New York: Springer.

Taflove, A., and S. Hagness. 2000. Computational electrodynamics: The finite-difference time-domain method. Boston, MA: Artech House.

Theuer, M., G. Torosyan, C. Rau, R. Beigang, K. Maki, C. Otani, and K. Kawase. 2006. Efficient generation of Cherenkov-type terahertz radiation from lithium niobate crystal with a silicon prism output coupler. Applied Physics Letters 88:071122–1–071122–3.

Velychko, L., and Y. Sirenko. 2009. Controlled changes in spectra of open quasi-optical resonators. Progress Electromagnetics Research B 16:85–105.

Yevdokymov, A. 2013. Diffraction radiation antennas. Fiz. Osnovy Priborostr. 2 (1):108–25. (in Russian).